Global Sensitivity Analysis Applied to Drying Models for One or a Population of Granules

Séverine Thérèse F. C. Mortier
BIOMATH, Dept. of Mathematical Modelling, Statistics and Bioinformatics, Faculty of Bioscience Engineering, Ghent University, Coupure Links 653, Ghent 9000, Belgium

Laboratory of Pharmaceutical Process Analytical Technology, Dept. of Pharmaceutical Analysis, Faculty of Pharmaceutical Sciences, University of Ghent, Harelbekestraat 72, Ghent 9000, Belgium

Krist V. Gernaey
Dept. of Chemical and Biochemical Engineering, Center for Process Engineering and Technology, Technical University of Denmark, Lyngby 2800 Kgs., Denmark

Thomas De Beer
Laboratory of Pharmaceutical Process Analytical Technology, Dept. of Pharmaceutical Analysis, Faculty of Pharmaceutical Sciences, University of Ghent, Harelbekestraat 72, Ghent 9000, Belgium

Ingmar Nopens
BIOMATH, Dept. of Mathematical Modelling, Statistics and Bioinformatics, Faculty of Bioscience Engineering, Ghent University, Coupure Links 653, Ghent 9000, Belgium

DOI 10.1002/aic.14383
Published online February 5, 2014 in Wiley Online Library (wileyonlinelibrary.com)

The development of mechanistic models for pharmaceutical processes is of increasing importance due to a noticeable shift toward continuous production in the industry. Sensitivity analysis is a powerful tool during the model building process. A global sensitivity analysis (GSA), exploring sensitivity in a broad parameter space, is performed to detect the most sensitive factors in two models, that is, one for drying of a single granule and one for the drying of a population of granules [using population balance model (PBM)], which was extended by including the gas velocity as extra input compared to our earlier work. β_2 was found to be the most important factor for the single particle model which is useful information when performing model calibration. For the PBM-model, the granule radius and gas temperature were found to be most sensitive. The former indicates that granulator performance impacts drying behavior, the latter is informative with respect to the variables that primarily need to be controlled during continuous operation. In addition, several GSA techniques are analyzed and compared with respect to the correct conclusion and computational load.
 AIChE J, 60: 1700–1717, 2014
Keywords: global sensitivity analysis, techniques, drying model, population balance model, pharmaceuticals

Introduction

Pharmaceutical fluidized bed drying process

Today, the pharmaceutical industry mainly uses batch-wise production systems[1]; however, there is a clear trend to shift toward continuous processing. Continuous production systems have several advantages, such as increased flexibility and efficiency, avoiding scale-up issues, reducing cycle times, and so forth.[1–3] However, these advantages require a confident control strategy of the process to safeguard the product quality at all times. In this respect, batch processes mostly rely on offline time-consuming measurements, whereas continuous systems could make use of online measurement tools and real-time adaptation of sensitive input variables. The latter requires thorough process knowledge and insight. Mechanistic models are a useful tool to obtain detailed information about the process and, hence, to support development of control strategies.

The production of pharmaceutical tablets consists of several consecutive steps. The process starts with the blending of the individual components (excipients and active pharmaceutical ingredient), after which a granulation step is performed. If a wet granulation technique is chosen, then the wet granules must undergo a drying step prior to the tabletting step.[3] In this contribution, the drying step of a full continuous from-powder-to-tablet manufacturing line, that is, the ConsiGma™ (Collette™, GEA Pharma Systems, Wommelgem, Belgium), is the process under study. The drying unit is a six-segmented fluidized bed, which operates in a semi-continuous mode.

Correspondence concerning this article should be addressed to S. T. F. C. Mortier at severine.mortier@ugent.be.

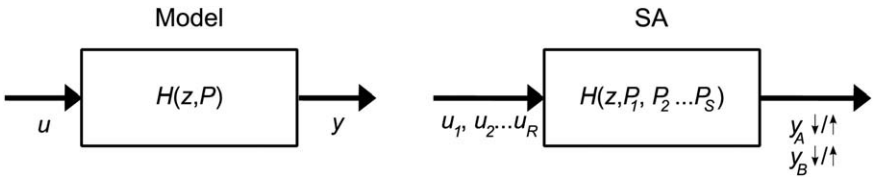

Figure 1. Representation of a model—Sensitivity analysis.

In the next part of the introduction, the focus is made on the use of a sensitivity analysis during model building. A section is added to introduce the symbols and the notation used in this article. Furthermore, several sampling techniques are discussed which are used during a global sensitivity analysis (GSA). In the last part of the introduction, the GSA techniques used in this contribution are described in detail.

Sensitivity analysis and its added value to mathematical modeling

Models are becoming increasingly important to gather knowledge about processes, but also to support decision-making processes. Good practice in model development and application is needed to obtain credible results, valuable information, and insight in the process. Ten basic steps of good, disciplined model practice are described by Jakeman et al.[4] During model building, uncertainty and sensitivity analysis are important steps. In an uncertainty analysis, the uncertainties in input variables are propagated through the model to compute the uncertainty on the output. A sensitivity analysis is the study of how the uncertainty in the output of a model (numerical or otherwise) can be apportioned to different sources of uncertainty in the model input (or model structure, parameters).[5] This provides useful information if one is to reduce the model output uncertainty.

In Figure 1, a schematic representation of a model is presented. A model H computes one or more outputs y with a number of input variables u and parameters P, respectively, indicated as R and S in Figure 1. Performing a sensitivity analysis means that different values for the inputs and parameters are investigated. In the following, the combination of inputs and parameters used in the analysis are referred to as factors. Depending on the way a factor appears in the model, the output can decrease or increase in a more or less significant way.

A first differentiation can be made between the local, one factor at a time (OAT) and the global methods for sensitivity analysis (Figure 2). The local methods focus on the sensitivity around one point in the factor space. An example in the two-dimensional (2-D) factor space is presented in Figure 2. To calculate the sensitivity in an OAT analysis, the central difference scheme is most often used

$$\frac{\partial y(t)}{\partial x_i} = \frac{y(t, x_i + \xi x_i) - y(t, x_i - \xi x_i)}{2\xi x_i} \tag{1}$$

with $y(t, x_i)$ the output variable, x_i the nominal value of the perturbed factor, and ξ the perturbation factor. The perturbation factor should be chosen adequately, as a too low value lead to numerical issues and too high values leads to potentially inaccurate sensitivities due to model nonlinearity (given the factor is nonlinear in the model). The drawback of this local method is that sensitivity can be very different at different locations in the factor space which limits the conclusions to the chosen point only. The OAT technique simply varies one factor at a time, and is a pseudoglobal technique. The difference between the values for the factor is much larger compared to the local sensitivity analysis, but as only one factor is varied, the technique is not able to detect interactions among the factors. The GSA explores the whole factor space and as such much more information can be obtained.

Several methodologies to test the sensitivity are available in the literature.[5–7] The GSA techniques can be roughly divided into different types; quantitative approaches (regression-based, rank-based regression, variance-based, moment-independent techniques, meta-modeling, techniques based on Monte Carlo sampling, etc.), qualitative techniques,[8] or methods with regional properties.[9] Conversely, there are the screening techniques, for example, the OAT screening techniques. An estimate of partial derivatives is used to detect the effect of one uncertain factor on the output while the other factors are fixed. In this sense, there are also the so-called local sensitivity measures.[10] These methods require a

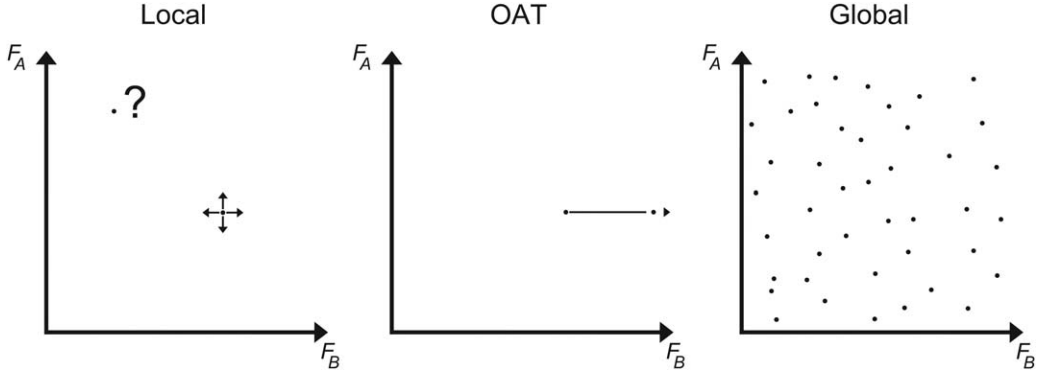

Figure 2. Different types of sensitivity analysis.

lower number of model evaluations, which is interesting when a high number of factors is present in the model.[11] However, interactions between factors can not be assessed as no more than one input is simultaneously changed.[10] Morris[12] proposed a screening method for models with a high number of uncertain factors and/or an expensive computation of the model output.[12] The Morris screening is an interesting tool to use as a first step when dealing with complex models.

There are several incentives to perform a sensitivity analysis:

- Increased understanding of the model behavior: What is the quantitative impact of decreasing or increasing a factor F on the output $y : F \uparrow \Rightarrow y \uparrow$ or $\downarrow$ (or a nonsensitive output).
- Model calibration: Based on the sensitivity of the factors it can be decided which factor should preferably be estimated using the experimental data. If a factor is more sensitive, the factor should be changed less to achieve a better description of the experimental data. In contrast, if a factor is not sensitive then it is impossible to estimate that factor based on the available data.
- Model reduction: The presence of nonsensitive parameters in the model can be questioned. Such parameters can be eliminated eventually when building a reduced model.
- Prediction uncertainty: If the model has an uncertain sensitive parameter, the output will also be uncertain. When one aims to reduce output uncertainty, focus should be on these parameters.

Symbols and Notation. The model of interest computes a scalar output y, which is required for most sensitivity analysis methods, based on k factors $(x_1, x_2, \ldots, x_k)$ $(y=H(\boldsymbol{x}))$, where these factors can be input variables (u) and/or parameters (P) (Figure 1). A computational experiment consists of N runs, meaning that N output values are generated. Given an experimental design, the jth row of the design matrix $\boldsymbol{X}$ ($N \times k$-matrix) is the set of factor values (x) for the jth run. X_i denotes a vector with values for factor i and $\boldsymbol{X}_{\sim i}$ the $N \times (k-1)$-matrix with all factors except X_i. Y is the vector with the scalar outputs.

Sampling Techniques. Performing a sensitivity analysis requires a set of factor values for each of the input factors that are considered in the sensitivity analysis. For this purpose, different sampling techniques are available, which sample values for the input factors with an interval. The interval used in the analysis can be chosen based on expert knowledge; for example, the experimental and/or physical limitations of the input variables. For parameters, the range can also be fixed by performing a literature study or by choosing realistic values. Random numbers or standard random numbers is the most basic form of probability sampling. It means that independent values of the random factor are uniformly distributed over the entire interval that is to be sampled. Pseudorandom numbers are numbers computed using a specific algorithm, but satisfying an accepted set of tests to mimic a truly random natural process.[13,14] In Monte Carlo computations, the values for the factors are replaced by various pseudorandom numbers, pseudorandom sampling is also known as pseudo-Monte Carlo sampling.[14] An advantage of pseudorandom sampling is the ease of implementation, however, the disadvantage is that large regions of the design space are not explored.[14] Stratified Monte Carlo sampling generates a more uniform sampling of the design space, because each interval is subdivided into bins.[15] The bins have an equal size if all variables have a uniform probability distribution. A better coverage of the design space and the flexibility to choose the number of subintervals are advantages. In some methods, the option exists to use a different number of bins for each interval.[14] For stratified samples, it is recommended that there are two bins for each variable, and as such there are at least 2^k samples generated. For expensive models or models with large k, this is a serious drawback. Latin hypercube sampling (LHS) sampling is a type of stratified sampling.[16,17] LHS is based on the idea of a Latin square meaning that there is only one sample in each row and each column.[18] In each interval, one value is selected at random with respect to the probability density in the interval. The N values for the different factors are then paired with each other in a random manner based on a pseudorandom number generator. The drawback is that the method is one-dimensional (1-D) and does not provide good uniformity over the whole volume of a k-dimensional unit hypercube.[16] The possible correlation between the variables is another deficiency, which can be compensated by using the correlation control method proposed by Iman and Conover (1982). When quasirandom sequences are used, also called low-discrepancy sequences, it is called a quasi-Monte Carlo simulation. The term "low discrepancy" means that the discrepancy between the distribution of generated points and a distribution with equal proportions of each subcube of a uniform partition of the hypercube is minimized. Several quasirandom sequences have been described in literature; Sobol,[19] Halton,[20] Faure,[21] Hammersley,[22] and so forth. The objective of these quasi-Monte Carlo methods is that they ensure even coverage and normally have a faster order of convergence. Quasirandom sequences are deterministic sequences; the position of previously sampled points is known and the construction of the samples is done in such a way to avoid the presence of gaps and clusters.[23,24] There are three characteristics of the commonly used Sobol' quasirandom sequences; (1) best uniformity of the generated distribution if $N \rightarrow \infty$, (2) good distribution for small initial sets, and (3) a very fast algorithm.[24,25]

Morris Screening. Morris Screening, also known as the original elementary effect (EE) method, is used to determine the factors which are (1) negligible, (2) linear and additive, or (3) nonlinear or (4) involved in interactions with other inputs. Two sensitivity measures are computed for each input; μ and σ. μ, an (absolute) measure of central tendency, determines the "overall" influence of the factor, whereas σ, a measure of spread, is important to detect the higher order effects of the factor, that is, nonlinear and/or interactions with other parameters.[12]

Several individually randomized OAT experiments form the experimental design. It is assumed that x_i is scaled (values in the interval [0,1], uniformly distributed), which is a commonly used approach within sensitivity analysis. The method computes for each factor a number of incremental ratios, which are called the EEs. The method is restricted to a region of experimentation ω, which is a regular k-dimensional p-level grid, as each factor is assumed to vary across p selected levels in the input factor space.[12]

The EE of the ith factor is defined as

$$d_i(\boldsymbol{x}) = \frac{[y(x_1, x_2, \ldots, x_{i-1}, x_{i+\Delta}, x_{i+1}, \ldots, x_k) - y(\boldsymbol{x})]}{\Delta} \quad (2)$$

with Δ a predetermined multiple of $1/(p-1)$. The finite distributions F_i of the calculated EEs for input i are obtained

by randomly sampling different factors from ω, that is, $d_i(\boldsymbol{x}) \sim F_i$. The number of EEs for each F_i is $p^{k-1}[p-\Delta(p-1)]$. To ensure at least a certain symmetric treatment of inputs, although the design strategy does not guarantee equal-probability sampling from each F_i, p is chosen even and Δ as $p/[2(p-1)]$. Morris proposed an efficient design that constructs r trajectories of $(k+1)$ points in the input space, each providing k EEs, one per input factor. The sensitivity measures are estimated with these r EEs from each F_i. The total number of runs is thus $r(k+1)$.[12]

$\boldsymbol{x}$ produces a simple random sample, and with this design matrix the output y is computed which is used for the calculation of the sample mean ($\bar{d}_i$) and variance (S_i^2) of the observed EEs for input i. These two measures are unbiased estimators of the mean and variance of F_i, and the standard error of the mean can be estimated as $\mathrm{SEM}_i = S_i/\sqrt{r}$.[12]

Campolongo et al. described the use of μ^*, which is the estimate of the mean of the distribution of the absolute values of the EEs, because for a complex model with several inputs and outputs the simultaneous use of the two sensitivity measures may be inefficient. μ^* is enough for a reliable ranking of the factors. When the model is nonmonotonic, μ^* solves the problem of the effects of opposite signs, however, there is a loss of information on the sign of the effect. A high value for μ and μ^* indicates that the sign of the effect is always identical; suggesting a monotonic output function. A low value for μ combined with a high value for μ^* occurs when the other factors lead to a variation in sign of the output deviations.[11]

Contribution to Sample Mean/Variance Plot. Graphical sensitivity tools, being qualitative techniques, are interesting to detect the relationship between uncertain model factors and model outputs.[26] The contribution to sample mean (CSM) plot was developed by Sinclair in 1993,[27] and further developments were made by Bolado-Lavin et al.[28] In this tool, a random sample of the factors is used for the analysis. An extension toward the CSM plot was made by Tarantola et al.[26] by introducing the contribution to sample variance (CSV) plots. A lot more information can be obtained by the (CSV) compared from the standard sensitivity indices (see further) when investigating input–output relationships. The standard indices are helpful to detect the most important input factor, however, no information is obtained about how to reduce the range of uncertainty of the important input factor for a given target reduction of the output variance.[26] An advantage of the graphical tools is the low number of simulations which are required to draw conclusions compared to, for example, Monte Carlo-based methods.

The CSM for an input X_i is defined by

$$\mathrm{CSM}_{X_i}(q) = \frac{1}{E(Y)} \int_{-\infty}^{\infty} \ldots \int_{-\infty}^{\infty} \int_{-\infty}^{F_i^{-1}(q)} \prod_{i=1}^{k} p_i(X_i) \times H(X_1, X_2, \ldots, X_k) dX_i dX_1 \ldots dX_{i-1} dX_{i+1} \ldots dX_k \quad (3)$$

$$E(Y) = \int_{-\infty}^{\infty} \ldots \int_{-\infty}^{\infty} \prod_{i=1}^{k} p_i(X_i) H(X_1, X_2, \ldots, X_k) dX_1 \ldots dX_k \quad (4)$$

with $q \in [0,1], E(Y)$ the mean value of the model output, $F_i^{-1}(q)$ the inverse cumulative distribution of X_i at quantile q and p_i the probability density function. The $\mathrm{CSM}_{X_i}(q)$ is plotted as function of q, representing a fraction of the distribution range X_i. $\mathrm{CSM}_{X_i}(q)$ is the fraction of the output mean which corresponds to the values of X_i smaller or equal than its q-quantile. By definition $\mathrm{CSM}_{X_i}(0) = 0$ and $\mathrm{CSM}_{X_i}(1) = 1$.[26,28]

The CSV for factor i is defined as

$$\mathrm{CSV}_{X_i}(q) = \frac{1}{V(Y)} \int_{-\infty}^{\infty} \ldots \int_{-\infty}^{\infty} \int_{-\infty}^{F_i^{-1}(q)} \prod_{i=1}^{k} p_i(X_i) \times (H(X_1, X_2, \ldots, X_k) - \boldsymbol{E}(Y))^2 dX_i dX_1 \ldots dX_{i-1} dX_{i+1} \ldots dX_k \quad (5)$$

$$V(Y) = \int_{-\infty}^{\infty} \ldots \int_{-\infty}^{\infty} \prod_{i=1}^{k} p_i(X_i) \times (H(X_1, X_2, \ldots, X_k) - E(Y))^2 dX_1 \ldots dX_k \quad (6)$$

with $V(Y)$ the variance of the model output. The CSV is calculated using a constant mean $E(Y)$ over the full range of all factors. CSV is plotted in a similar way as CSM.

When the curve of the CSM and the CSV is near the diagonal, this means that the contribution to the mean or the variance is equal throughout the full range of the factor.

Regression-Based and Rank-Based Regression. For the performance of a sensitivity analysis several Monte Carlo-based techniques are available.[29] The space of the input factors is sampled and the relationship between the model output and input factors is analyzed via standardized regression coefficients (SRCs), correlation coefficients, partial correlation coefficient, or correlation ratios. However, the assumptions of linearity or monotonic relationship are serious limitations, especially for complex models.[30] Most popular in this group are the SRCs, and these measures are based on a linear regression model and not on the original output. For this method, it is assumed that no correlation is apparent between the different input factors. If one assumes that the model has an error-free linear form, the following is valid[8]

$$Y = \sum_{i=1}^{k} \Omega_i X_i \quad (7)$$

with Ω_i the fixed coefficients and X_i the independent factors which are normally distributed [$X_i \sim N(\bar{x}_i, \sigma_{X_i})$ with $\bar{x}_i = 0$ for $i = 1, 2, \ldots, k$ (where $\bar{x}_i$ and σ_{X_i} are, respectively, the mean and the standard deviation of the factor)]. Additional assumptions are

$$\sigma_{X_1} < \sigma_{X_2} < \cdots < \sigma_{X_k} \quad (8)$$

$$\Omega_1 > \Omega_2 > \cdots > \Omega_k \quad (9)$$

The assumption mentioned in Eq. 9 is because of Eq. 8. Because the independent variables are normally distributed, the output variable Y is also normally distributed, and the standard deviation of the output σ_Y becomes

$$\sigma_Y = \sqrt{\sum_{i=1}^{k} \Omega_i^2 \sigma_{X_i}^2} \quad (10)$$

If the relative importance of X_i on the output variable Y is of interest, the partial derivative of Y to X_i is most often taken

$$S_{X_i}^d = \frac{\partial Y}{\partial X_i} \quad (11)$$

which yields for the linear model $S_{X_i}^d = \Omega_i$. However, this is not really reasonable, because this means that the ordering of the factors by importance would be

$$X_1 > X_2 > \cdots > X_k \tag{12}$$

Equation 11 can be improved by normalizing the derivative using the input–output standard deviations

$$S_{X_i}^{\sigma} = \frac{\sigma_{X_i}\partial X}{\sigma_X \partial X_i} = \Omega_i \frac{\sigma_{X_i}}{\sigma_Y} \tag{13}$$

If Eq. 13 is combined with Eq. 10, then it can be concluded that

$$\sum_{i=1}^{k} \left(S_{X_i}^{\sigma}\right)^2 = 1 \tag{14}$$

The use of the normalized equation is a good way to rank the different input factors based on sensitivity. It depends both on σ and Ω, just as it should, and second, the sensitivity measures are normalized to one.

This is the reason why after performing a Monte Carlo simulation, the output (Y) at a specific point in time of the simulation is processed using a linear regression.[31] This linear regression is performed on the scaled output and scaled degrees of freedom (autoscaling: scaling by first subtracting the mean followed by division by the standard deviation)

$$Y_{(j)} = b_0 + \sum_{i=1}^{k} b_{X_i} X_i^{(j)} \tag{15}$$

with $Y_{(j)}$ the output for one simulation, $X_i^{(j)}$ are the degrees of freedom used in this simulation and b_0, b_{X_i} are, respectively, the intercept and linear coefficients of the linear model that is constructed. The coefficients b_0 and b_{X_i} are determined by solving a straightforward least squares problem, based on the squared differences between the output values produced by the regression model and the actual model output produced by Monte Carlo simulation. Asymptotically, $\hat{b}_0 \cong 0$ and $\hat{b}_{X_i} \cong \Omega_i$ for $i=1,2,...,k$. Besides these coefficients, their standardized equivalents $\hat{\beta}_{X_i}$ (the SRC) are determined as

$$\hat{\beta}_{X_i} = \hat{b}_{X_i}\sigma_{X_i}/\sigma_Y \cong \Omega_i \sigma_{X_i}/\sigma_Y \tag{16}$$

Comparing Eq. 16 with Eq. 13, it can be proven that $\hat{\beta}_{X_i}$ coincides with $S_{X_i}^{\sigma}$ for linear models. Therefore, for linear models

$$\sum_{i=1}^{k} \left(S_{X_i}^{\sigma}\right)^2 = \sum_{i=1}^{k} \left(\hat{\beta}_{X_i}\right)^2 = 1 \tag{17}$$

If the model is nonlinear, both measures ($\hat{\beta}_{X_i}$ and $S_{X_i}^{\sigma}$) will be different, but the β's will be a more robust and reliable measure of sensitivity, even for nonlinear models. β's take the entire space of input factors into account, which is advantageous over $S_{X_i}^{\sigma}$. To ensure a reliable value for β, N should be large compared to k. The $\sum_{i=1}^{k} (\hat{\beta}_{X_i})^2$ equals the fraction of linearity of the model, more precisely known as the coefficient of determination, R_Y^2, which is equal to the fraction of variance of the original data (Monte Carlo simulation results), explained by the regression model (Eq. 15).[31] This value should at least be 0.7 for SRC to be a valid technique. In fact, for all regression-based methods the ranking is good as long as R_Y^2 is close to 1, as a low value means that a large part of the model output variance is left unaccounted in the sensitivity ranking.[30,32] A low value for R_Y^2 can be tackled by applying a rank transformation of the output, the ranked output is then used for computing the corresponding rank sensitivity measures (standardized rank regression coefficient (SRRC), Spearman rank coefficient of correlation, partial rank correlation coefficient). However, this rank transformation is only valid for monotonic data.[30]

The disadvantage of these methods is that they are computationally expensive, because a lot of samples are required, however, after simulation of the model the analysis is fast, and all measures can be calculated using the same sample and model. The obtained coefficients can only be used to assess the importance of a given parameter, whereas the S_i and S_{Ti} can be considered as clues of parameter influence (more details about these indices can be found in the next section). This information is much more precise and more informative with respect to the model behavior. Homma and Saltelli indicated the latter as being superior compared to the information obtained from other GSA methods, and as such also compared to the information obtained by the regression-based techniques.[32]

Variance-Based Sensitivity Analysis. The variance-based methods are very popular nowadays, and the obtained indices are much more informative compared to the SRCs, which are discussed in the previous section. They are defined from the decomposition of the total output variance into the contribution of the input factors. Advantages are[5,24,30]:

- The analysis is independent of the model structure, no prior assumptions about the model output are taken
- The full range of variation/uncertainty of the input variables can be incorporated in the analysis
- The use of total sensitivity indices enables to quantify the overall interaction effects between factors
- The analysis can be performed on groups of inputs

The decomposition of the model output variance $V(Y)$ for independent input factors is

$$V(Y) = \sum_i V_i + \sum_i \sum_{j>i} V_{ij} + \cdots + V_{12...k} \tag{18}$$

where

$$V_i = V_{X_i}(E_{\boldsymbol{X}_{\sim i}}(Y|X_i)) \tag{19}$$

$$V_{ij} = V_{X_iX_j}(E_{\boldsymbol{X}_{\sim ij}}(Y|X_i,X_j)) - V_{X_i}(E_{\boldsymbol{X}_{\sim i}}(Y|X_i)) - V_{X_j}(E_{\boldsymbol{X}_{\sim j}}(Y|X_j)) \tag{20}$$

Division of both sides of Eq. 18 by $V(Y)$ yields

$$1 = \sum_i S_i + \sum_i \sum_{j>i} S_{ij} + \cdots + S_{12...k} \tag{21}$$

with S_i, S_{ij} the sensitivity indices for first and higher order effects. S_i is normalized, because

$$V(Y) = V_{X_i}(E_{\boldsymbol{X}_{\sim i}}(Y|X_i)) + E_{X_i}(V_{\boldsymbol{X}_{\sim i}}(Y|X_i)) \tag{22}$$

and $V_{X_i}(E_{\boldsymbol{X}_{\sim i}}(Y|X_i))$ varies between zero and $V(Y)$. This variance decomposition has $2k-1$ terms, but in general only the k first-order effects (S_i) and the k total effects (S_{Ti}) are calculated

$$S_{Ti} = \frac{E_{\boldsymbol{X}_{\sim i}}(V_{X_i}(Y|\boldsymbol{X}_{\sim i}))}{V(Y)} = 1 - \frac{V_{\boldsymbol{X}_{\sim i}}(E_{X_i}(Y|\boldsymbol{X}_{\sim i}))}{V(Y)} \tag{23}$$

S_i indicates the actual fraction of variance accounted for by each factor.[32] S_{Ti} represents the total effect of factor i, that is, the sum of the first-order effect and all interactions with other factors. Another interpretation of the indices is in

terms of the expectation of the reduction of the variance, but this is only valid when the factors are not independent.[33] $V_{X_i}(E_{\boldsymbol{X}_{\sim i}}(Y|X_i))$ is the expected reduction in variance when X_i would be fixed and $E_{\boldsymbol{X}_{\sim i}}(V_{X_i}(Y|\boldsymbol{X}_{\sim i}))$ is the expected residual variance if all factors are fixed except X_i, because $V_{\boldsymbol{X}_{\sim i}}(E_{X_i}(Y|\boldsymbol{X}_{\sim i}))$ is the expected value of the variance reduction if all factors except X_i could be fixed.[34]

Different designs are known to calculate these sensitivity indices.[10,17] Saltelli et al.[34] proposed to approximate the estimator of V_i as

$$V_{X_i}(E_{\boldsymbol{X}_{\sim i}}(Y|X_i)) \approx \frac{1}{N}\sum_{j=1}^{N} f(\boldsymbol{B})_j\left(f(\boldsymbol{A}_{\boldsymbol{B}}^{(i)})_j - f(\boldsymbol{A})_j\right) \tag{24}$$

where $\boldsymbol{A}$ and $\boldsymbol{B}$ are $N \times k$-matrices of input factors and $\boldsymbol{A}_{\boldsymbol{B}}^{(i)}$ is a $N \times k$-matrix where column i comes from matrix B and the other columns are those of matrix A. This is an improvement of the estimator related to the use of quasi-Monte Carlo samples. For the estimate of S_{Ti}, the equation of Jansen[35] is used as proposed by Saltelli et al.[34] To obtain the best estimator for S_{Ti}, quasirandom number generation in the $\boldsymbol{A},\boldsymbol{A}_{\boldsymbol{B}}^{(i)}$ configuration and radial sampling are proposed.[34]

Also here, a rank transformation can be performed. However, the use of the rank is conceptually different compared to the rank transformation used in the regression-based techniques. Whereas the rank is essential for these analyses to tackle the problem of nonlinearity, for the sensitivity indices it is a matter of robustness. To obtain the same results with a different set of input factors, the rank-transformed version of the sensitivity indices is more suitable. But due to the forced linearization, the fraction of the total variance accounted for by the first-order indices increases.[32]

Objectives

In this contribution, two models are used for the GSA: (1) a model which describes the drying behavior of a single pharmaceutical granule[36] and (2) a population balance model (PBM) describing the drying behavior of a population of wet granules.[37] Both models are first briefly introduced in the section "Materials and Methods." Prior to the GSA analysis on the PBM-model the reduced model, described by Mortier et al.,[37] was extended with an extra degree of freedom, that is, the gas velocity, in order to be able to account for this factor in the GSA as well. Furthermore, for both models several GSA techniques are compared to investigate their performance. For the single particle drying model, the GSA is performed for all factors included in the model to investigate the influence of the factors on the drying time. The outcome of the GSA on the drying model can be used to perform a better model calibration.

The PBM-model is investigated through a GSA in order to improve the control of the drying process during continuous operation. The analysis is done on six factors and more details about the choice of the factors used in the GSA can be found in the section "Reduced drying model for the PBM-model." The objective of this sensitivity analysis is to investigate which factors have the largest influence on the distribution of the moisture content of the particles which is predicted by the PBM. This will provide useful information with respect to developing control strategies for this unit process when used in the continuous application.

Materials and Methods

Single particle drying model

The drying model under study consists of two submodels each describing a distinct drying phase.[36] The first drying phase entails the evaporation of water from the droplet free surface. The evaporation rate in this phase is given by

$$\dot{m}_v = h_D(\rho_{v,s} - \rho_{v,\infty})\boldsymbol{A}_{\mathrm{d}} \tag{25}$$

where $\dot{m}_v$ is the mass-transfer rate, h_D the mass-transfer coefficient, $\rho_{v,s}$ the partial vapor density near the droplet surface, $\rho_{v,\infty}$ the partial vapor density in the ambient air, and $\boldsymbol{A}_{\mathrm{d}}$ the surface area of the droplet. When the radius of the droplet equals the radius of the dry particle the second drying phase starts, in which two regions are formed: a wet core and a dry crust. In the second phase, the evaporation rate is given by

$$\dot{m}_v = -\frac{8\pi\epsilon^{\beta_1 e^{\beta_2 T_{\mathrm{g}}}} D_{v,\mathrm{cr}} M_{\mathrm{w}} p_{\mathrm{g}}}{\Re(T_{\mathrm{cr},s} + T_{\mathrm{wc},s})} \ln\left[\frac{p_{\mathrm{g}} - p_{v,i}}{p_{\mathrm{g}} - (\frac{\Re}{4\pi M_{\mathrm{w}} h_D R_{\mathrm{p}}^2}\dot{m}_v + \frac{p_{v,\infty}}{T_{\mathrm{g}}})T_{p,s}}\right] \tag{26}$$

with ε the crust porosity, $D_{v,\mathrm{cr}}$ the vapor diffusion coefficient (crust pores), M_{w} the molecular weight of the liquid, p_{g} the pressure of the drying agent, $T_{\mathrm{cr},s}$ and $T_{\mathrm{wc},s}$, respectively, the temperature of the crust outer surface and of the crust-wet core interface, $p_{v,i}$ and $p_{v,\infty}$, respectively, the partial vapor pressure at the crust-wet core interface and in the ambient air, h_D the mass-transfer coefficient, β_1 and β_2 two calibrated coefficients, R_{p} the particle radius, and T_{g} the temperature of the drying agent. The vapor, evaporated at the interface between the wet core and the dry crust, diffuses through the crust pores until it exits the pores, and forms a thin boundary layer over the particle surface. This vapor is removed through advection by the air flow. The complete drying model is extensively described by Mortier et al.[36]

The nominal values of the factors used in the model are mentioned in Table 1.

Most GSA techniques require a single value for the output y; for this purpose it was opted to choose the time to reach a moisture content of 1.4% as single output value (t_{proc}). The drying model contains 23 factors of interest.

In a first step, a Morris Screening was performed with these 23 factors, subsequently the 10 most sensitive factors were used for further analysis. Two different sampling techniques were used; LHS, proposed by McKay et al.,[17] and the Sobol sampling technique.[19]

Reduced drying model for the PBM-model

A reduced model for the drying of a single granule at different gas temperatures was described in detail by Mortier et al.[37] It was developed for the purpose of integrating it into a PBM as the original model is too complex. Here, an extension of the reduced empirical model is presented by introducing the gas velocity V_{g} in the first drying phase.[37] V_{g} was indicated as the second most significant degree of freedom, after the gas temperature T_{g}.[37] The selection of the significant degrees of freedom was based on a GSA on the single particle drying model using SRCs. The regression-based sensitivity analysis was done on five degrees of freedom.[37] The resulting empirical equation for the first drying phase is determined to be

Table 1. Factors Used in the GSA for the Single Particle Drying Model

Nr.	Factor	Nominal Value
1	$\boldsymbol{T_g}$	**55°C**
2	V_g	200 m3/h
3	$\boldsymbol{p_g}$	**101000 Pa**
4	$\boldsymbol{R_p}$	**0.6 mm**
5	Humidity	9%
6	$T_{p,0}$	25°C
7	ε	**0.05**
8	μ_{gas}	0.00002 kg/m/s
9	ρ_{gas}	1.2 kg/m3
10	k_{gas}	0.0285 W/m/K
11	$c_{p,gas}$	1009 kg/m^3
12	$\boldsymbol{M_w}$	**18.015e-3 kg/mol**
13	$\boldsymbol{\rho_{liquid}}$	**1000 kg/m^3**
14	$\boldsymbol{\rho_{solid}}$	**1525 kg/m^3**
15	$k_{droplet}$	0.07 W/m/K
16	k_{liquid}	0.63 W/m/K
17	k_{solid}	0.75 W/m/K
18	$c_{p,s}$	1252 kg/m^3
19	TWC	647.13 K
20	ϵ_{rs}	0.8
21	$\boldsymbol{\beta_1}$	**4912.4**
22	$\boldsymbol{\beta_2}$	**−0.024282**
23	$\boldsymbol{R_{w,0,fac}}$	**1.025**

Factors indicated in bold are used for all GSA techniques, whereas the others are only used for the Morris screening.

$$G^*_{r,1}(R_{w,nor}, T_g, V_g) = (v_1 V_g^2 + v_2 V_g + v_3)\, G_{r,1}(R_{w,nor}, T_g) \tag{27}$$

$$G_{r,1}(R_{w,nor}, T_g) = A + B R_{w,nor} + C\, e^{D R_{w,nor}} \tag{28}$$

$$R_{w,nor} = \frac{R_w - R_p}{R_{w,0} - R_p} \tag{29}$$

where v_1, v_2, and v_3 are empirical coefficients, A, B, C, and D are empirical coefficients, which are dependent on T_g and $R_{w,0}$ is the initial (wet) radius.[37] More details about the structure of the coefficients can be found in Mortier et al.[37] The coefficients for the first drying phase $G^*_{r,1}(R_{w,nor}, T_g, V_g)$ were optimized simultaneously with the coefficients of the original empirical function $G_{r,1}(R_{w,nor}, T_g)$ to reduce the error. The resulting coefficients are given in Table 2.

The behavior of the second drying phase is described by

$$G_{r,2}(R'_{w,nor}, T_g) = A' (R'_{w,nor})^{B'} + C' \left(1 + D' R'_{w,nor}\right)^{E'} + R'_f \left(A' 0.5^{B'} + C' (1 + D' 0.5)^{E'}\right) \tag{30}$$

$$R'_{w,nor} = \frac{R_w}{R_p} \tag{31}$$

with A', B', C', D', and R'_f empirical coefficients, dependent on T_g.[37]

PBM-model

The reduced model was used in a PBM-model.[38] The resulting population balance equation (PBE) is

$$\frac{\partial}{\partial t} n(R_w, t) + \frac{\partial}{\partial R_w} \dot{R}_w(R_w, Y)\, n(R_w, t) = 0 \tag{32}$$

with $n(R_w, t)$ the number density, Y the continuous phase vector, which includes T_g and V_g. $\dot{R}_w(R_w, Y)$ equals, respectively, $G^*_{r,1}(R_{w,nor}, T_g, V_g)$ and $G_{r,2}(R'_{w,nor}, T_g)$ for the first and the second drying phase. More details can be found in Mortier et al.[38] The method of characteristics, which uses a moving grid, is used to solve the PBE.[39] This solution method gave the best results taking both the accuracy and computational load into account.[38] A grid size of 100 was used for the calculations.

As most GSA techniques require one single value as output value for each Monte Carlo simulation, it was decided to perform two analyses. One on the standard deviation of the distribution at the end of the process (σ_d), and one on the mean of the distribution at the end (μ_d). Other output values can also be investigated, but as the product quality at the end of the process is the main point of interest for pharmaceutical production processes, these two output values seemed to be reasonable.

The factors used in the GSA are chosen based on the operation of the fluidized bed dryer of the ConsiGma™. The wet granules are fed into one of the six segments during a certain filling period t_{fil}, after which the next segment is filled. After the filling period, the wet granules are further dried, where the total drying time includes t_{fil} and is indicated as t_{dry}. This means that some granules are dried longer compared to others, that is, the drying time varies between t_{dry}-t_{fil} and t_{dry}. The factors used for the GSA are the gas temperature T_g, the gas velocity V_g, the particle radius R_p, the initial moisture content of the wet granules $R_{w,0,fac}$, t_{fil}, and t_{dry}. The range of the factors used in the simulations is presented in Table 3.

Results

Single particle drying model

Morris Screening. The 23 factors of the drying model are used for the Morris screening to differentiate in a first approach between the more and less sensitive factors. Subsequently, the less sensitive parameters are not taken into account in applying the other GSA methods. The range for the factors is chosen as 95–105% of the nominal value of the factors (Table 1). r is chosen as 10, so in total 240 simulations are performed. In Figures 3 and 4, the result is presented for, respectively, $\bar{d}_i$ and $\bar{d}^*_i$. Using $\bar{d}_i$ to detect the most important factors, it is obvious that factor 22 (β_2) and 1 (T_g) are the most important factors, followed by factor 21 (β_1) and 23 ($R_{w,0,fac}$) where the factor numbers correspond to

Table 2. Parameter Values for the Extended First Drying Phase (Coefficients which are Changed Compared to Mortier et al.[37] and the Extra Coefficients are Indicated in Bold).

a_1	−6.43e-15	b_1	1.45e-12	c_1	4.97e-12	d_1	0.0037	$\mathbf{v_1}$	**−1.28e-6**
a_2	−2.74e-12	$\mathbf{b_2}$	**−1.35e-10**	$\mathbf{c_2}$	**62.67**	d_2	−0.408	$\mathbf{v_2}$	**0.00238**
a_3	−5.28e-10	b_3	−3.99e-09	c_3	202.82	d_3	23.5	$\mathbf{v_3}$	**−0.427**
a_4	−7.24e-09	b_4	−2.57e-08	c_4	−3.05e-13				
a_5	−2.35e-07			c_5	36.43				
				$\mathbf{c_6}$	**96.29**				

Table 3. Factors Used in the GSA for the PBM-Model

Factor	Range
T_g	25–45°C
R_p	0.3–1.4 mm
V_g	200–400 m^3/h
$R_{w,0,fac}$	1.015–1.030
t_{fil}	60–400 s
t_{dry}	600–1800 s

the numbers mentioned in Table 1. In fact, there are eight inputs which are clearly separated from the other inputs, which have a mean and standard deviation close to zero. For the eight inputs with a mean significantly different from zero, the standard deviation is also clearly different from zero. These inputs appear to have effects that involve either curvature (nonlinear) or interactions. The result for $\bar{d}_i^*$ is comparable, also in this case the factors with the highest value for $\bar{d}_i^*$ are the factors 22 and 1. In fact, the ranking of the factors is identical for both techniques. As both cases gave the same result, this also means that the sign of the effect is always identical.

The low number of simulations required for this method is very attractive as a first screening method; however, it provides only qualitative sensitivity measures. The method ranks the input factors in order of importance, there is no quantification made to indicate how much a certain factor is more important than another.[40] Therefore, further analysis using other techniques is performed with the aim of obtaining more information about the 10 most sensitive factors resulting from this first screening.

Dotty Plots. Further analysis is done using the 10 most sensitive factors determined by the Morris screening. Dotty plots were created to gain insight in input–output relations. The scatter plots of the modeled output (t_{dry}), generated by the LHS sampling technique, are presented in Figure 5. Note that only the scatter plots where the influence is dependent on the value of the factor are presented. It is obvious that the drying time is higher for lower gas temperatures (Figure 5). The single particle drying model was calibrated earlier for β and an exponential relationship was introduced as a function of T_g, where two parameters were introduced (β_1 and β_2). When β decreases, the evaporation rate increases and the drying time will decrease. Based on Figure 5, it can

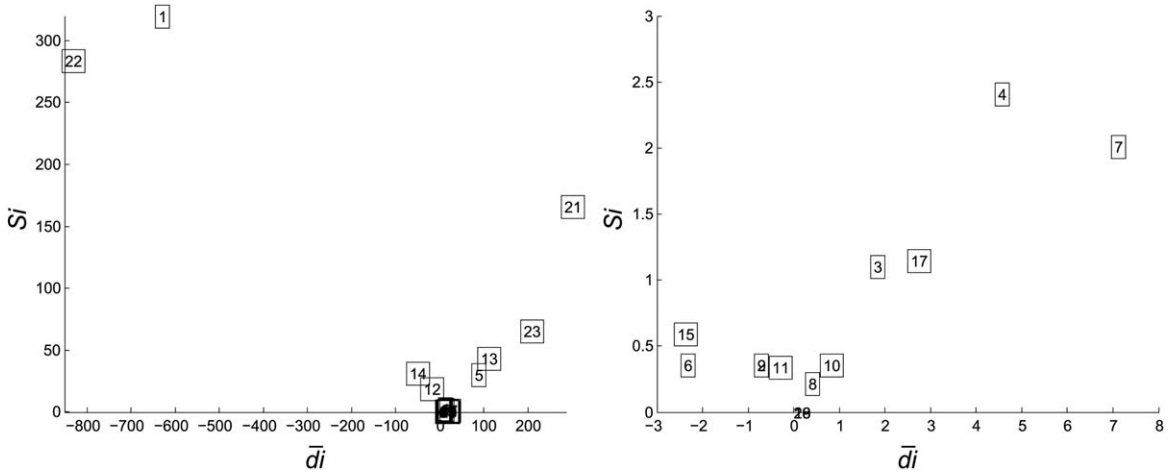

Figure 3. $\bar{d}_i$ and S_i for the Morris Screening of the single particle drying model with 23 factors (left) and a zoom of the area around the origin (right).

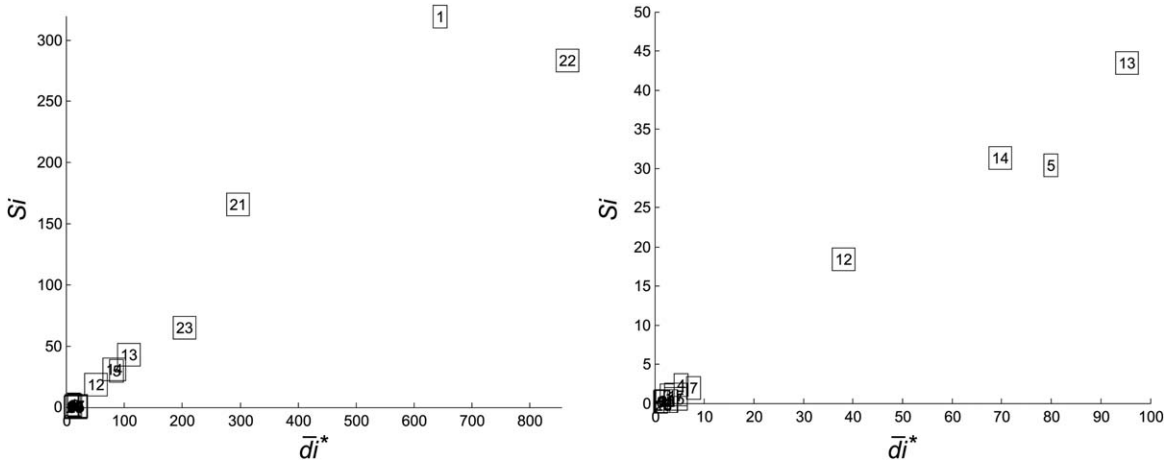

Figure 4. $\bar{d}_i^*$ and S_i for the Morris Screening of the single particle drying model with 23 factors (left) and a zoom of the area around the origin (right).

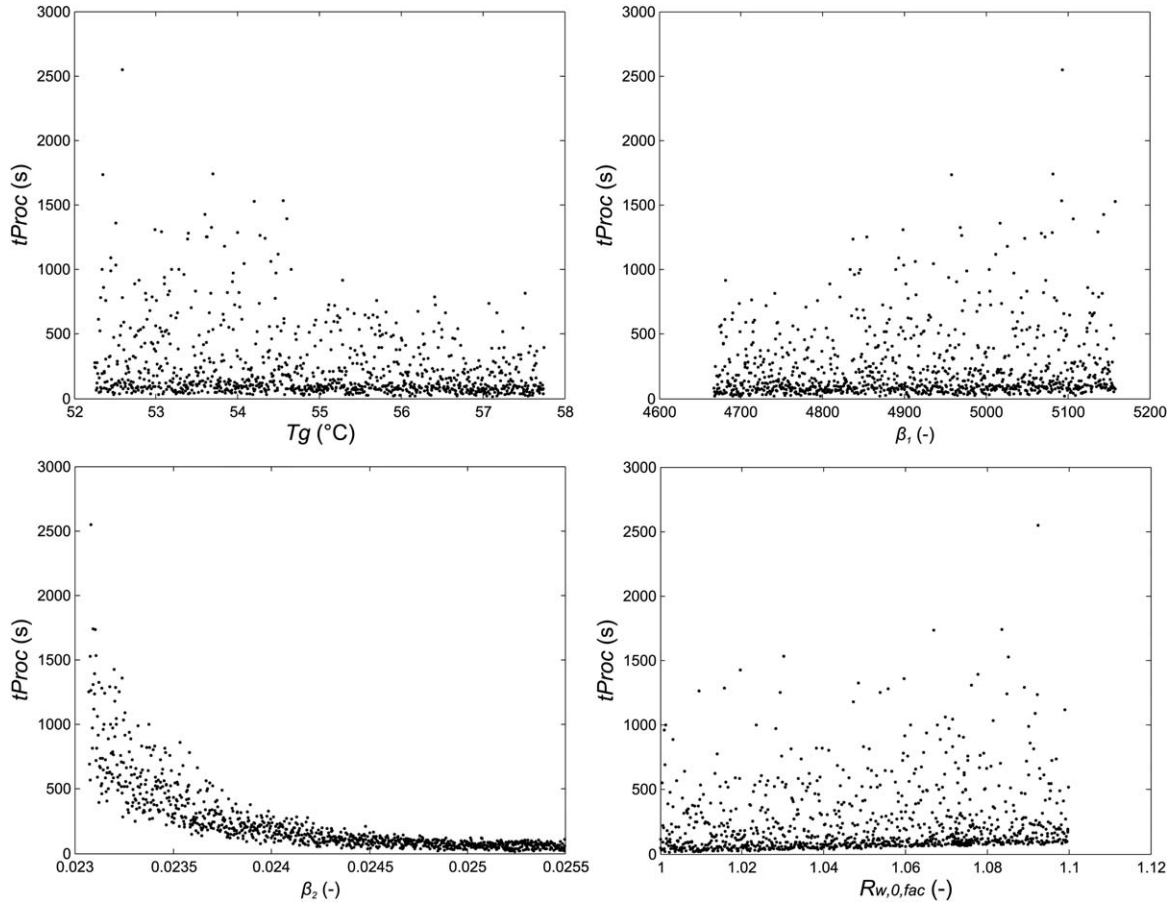

Figure 5. The scatter plots for the single particle drying model with $N = 1000$ using LHS sampling.

be concluded that the drying time increases for increasing values of β_1, as a consequence of the decreasing evaporation rate. The clearest trend was found for β_2. A high value for β_2 decreased the drying time enormously independent from the values of the other parameters. However, a low value for β_2 leads to more variation in drying time. This factor β_2 was included in the drying model during the calibration step,[36] but no physical explanation can be given for this particular dependence of β on the gas temperature. When $R_{w,0,fac}$ increases, it can be expected that the drying time will also increase.

Contribution to Sample Mean/Variance Plot. The analysis was done for 1000 simulations (N) using the LHS and the Sobol sampling technique. In Figure 6, the 2-D scatter plots of the p_g and T_g are presented for the LHS and Sobol sampling methodology. The difference between both methods is obvious, whereas the pattern for the LHS design looks

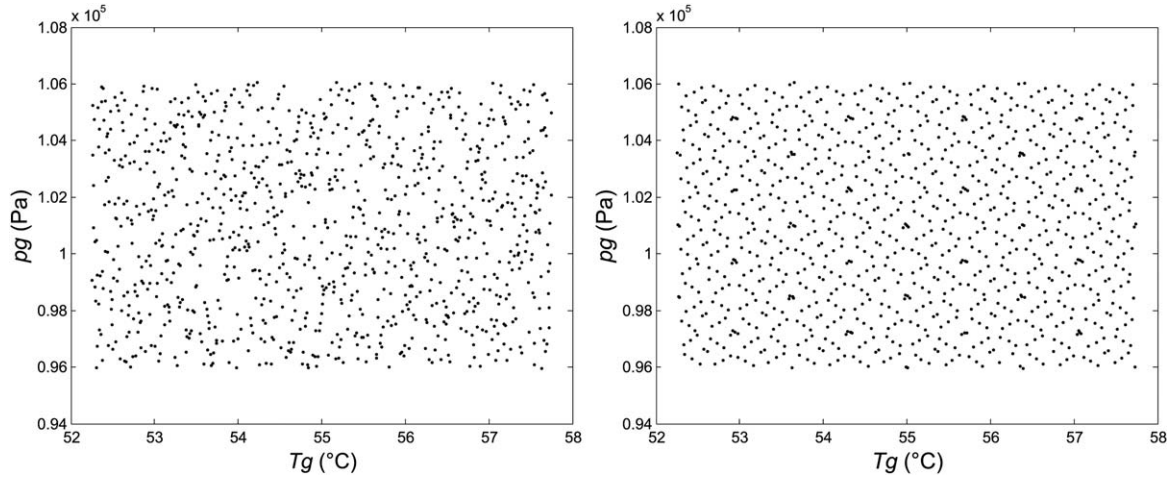

Figure 6. The 2-D scatter plots for p_g and T_g for both sampling methodologies for the single particle drying model (LHS on the left, Sobol on the right).

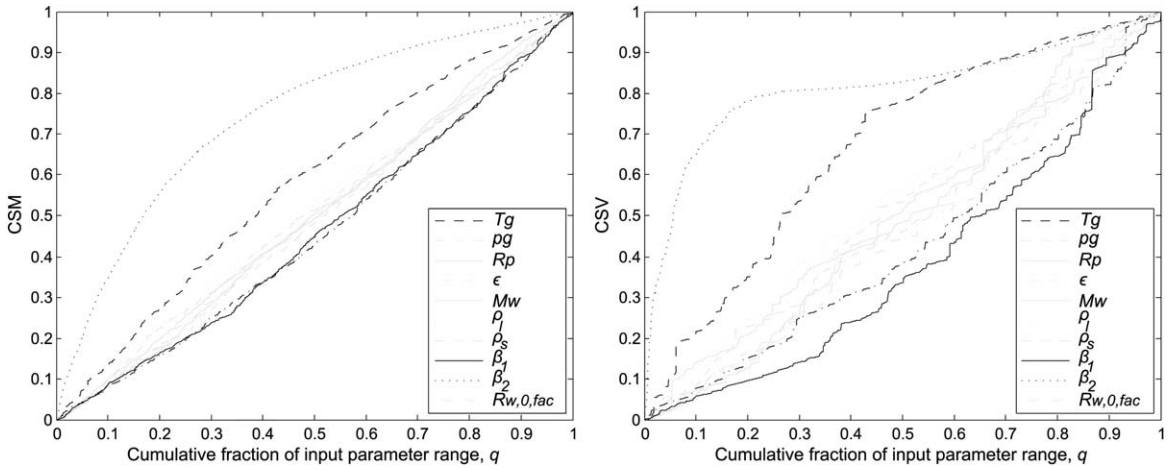

Figure 7. The CSM (left) and CSV (right) plot for the single particle drying model with $N = 1000$ using LHS sampling.

The factors which have less influence are indicated in gray.

random; the design matrix using the Sobol generator is quite regular.

In Figure 7, the CSM and the CSV plot are presented. β_2 deviates obviously the most from the bisector, and as such it can be concluded that this is the most important factor. T_g, β_1, and $R_{w,0,fac}$ are subsequently the most sensitive factors. Some curves cross the bisector multiple times. Bolado-Lavin et al.[28] suggested to calculate the sum of the absolute maximum distances from the diagonal and use this value to rank the factors. The concavity of the CSM plot indicates the relation between the input and the output when this relation is monotonic. A positive monotonic relation leads to a curve below the bisector and a negative monotonic relation to a curve above. This means that for increasing values of β_2 the drying time decreases, which was also clear from Figure 5. In the CSV plot, β_2 deviates the most from the diagonal, indicating that the output variance is the most unevenly distributed for this parameter. This is confirmed by looking at the scatter plots (Figure 5). For most factors, the width of the output is equal over the whole range, whereas for β_2 the width is much smaller for high values compared to lower values. Also for T_g, β_1, and to a lesser extent $R_{w,0,fac}$ the width is dependent on the value of the factor, whereas for the other six factors the variance is more evenly distributed over the range of the input.

The scatter plots using the Sobol design matrix are similar to the scatter plots using the LHS sampling method, and are not shown. In Figure 8, the CSM and the CSV plot are visualized for the Sobol sampling method. In general, the same conclusions can be drawn as for the LHS sampling, but some small deviations can be detected. The curve of $R_{w,0,fac}$ deviates less from the diagonal compared to the LHS sampling method. The same is valid for the CSV plot, and here, ρ_{liquid} and R_p have an even larger influence on the variance.

Regression-Based Sensitivity Analysis. This method is based on 1000 samples again generated by LHS and Sobol sampling. Using the raw output data, simulated using LHS sampling, the R_Y^2 is only 0.62, however, the rank transformation increases the coefficient of determination (0.95) significantly (Table 4). The rank transformation is performed by ranking the output and use the rank number instead of the actual output value. In fact, this means that the SRCs are not able to provide a reliable ranking of the input factors. The

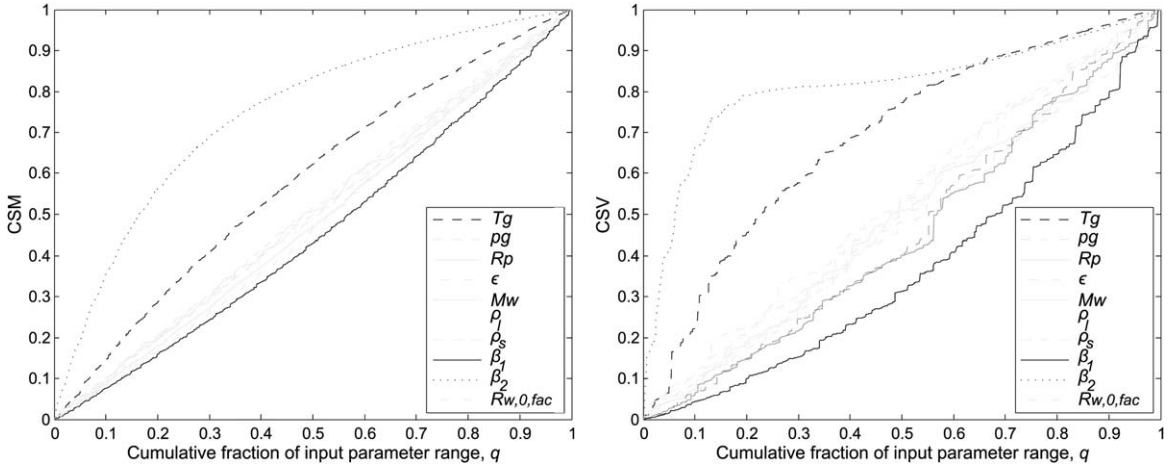

Figure 8. The CSM (left) and CSV (right) plot for the single particle drying model with $N = 1000$ using Sobol sampling.

The factors which have less influence are indicated in gray.

Table 4. Results of the Regression-Based Method for the Single Particle Drying Model

Parameter	SRC	SRRC
T_g	0.2329	0.2121
p_g	0.0370	0.0727
R_p	0.0119	0.0230
ε	0.0262	0.0187
M_w	0.0341	0.0753
ρ_{liquid}	0.0351	0.0424
ρ_{solid}	0.0089	0.0057
β_1	0.1185	0.1108
β_2	0.7293	0.9015
$R_{w,0,fac}$	0.1242	0.2438
R_Y^2	0.62	0.95

linear regression for both methods is presented in Figure 9. The difference between both methods is obvious, whereas the data points of the raw values show a more exponential behavior, the data points resulting from rank transformation are clearly more linear. The linear model outputs of the rank transformed data points follow the linear trend of the simulated model outputs. The linear regression without performing an *a priori* rank transformation is not able to describe the simulated output of the drying model. The difference between both R_Y^2 values is a useful indicator for the nonlinearity of the model. The SRRCs have no quantitative value compared to the SRCs, but can only be used to rank the input factors.

Both the SRC and the SRRC is the largest for β_2, but for further ranking the results between the coefficients based on raw values and rank transformation are different (Table 4). The order of significance is switched for T_g and $R_{w,0,fac}$. It is remarkable that the ranking is different compared to the ranking obtained by the CSM plot.

The result, using Sobol to generate the input factors, is presented in Figure 10, together with the result of the LHS sampling scheme. The R_Y^2 is nearly unchanged when performing the linear regression on the data generated using Sobol sampling compared to LHS. For the most sensitive parameters, that is, those with the highest values, both sampling schemes give approximately the same result. On less significant factors, for example, R_p or M_w, the difference between both sampling schemes is more pronounced.

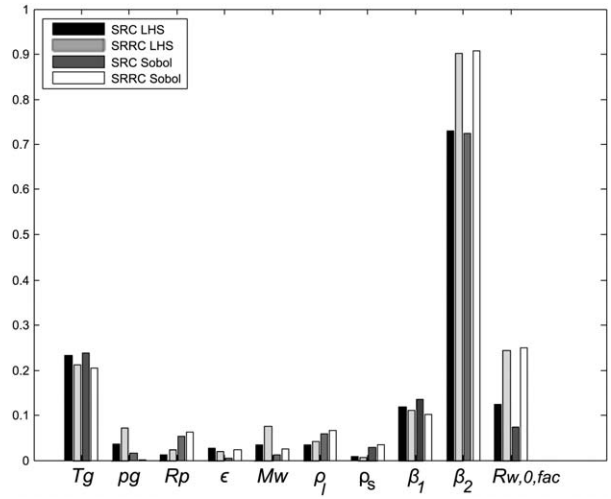

Figure 10. Results of the regression-based GSA for LHS and Sobol as sampling techniques for the single particle drying model.

Variance-Based Sensitivity Analysis. The sensitivity indices are computed based on the method proposed by Saltelli et al.[34] In Table 5, the values for the S_i and S_{Ti} are presented. It is important to mention that negative values for the sensitivity indices are theoretically impossible, as the indices are a ratio of variances. But the relative importance of the factors is not affected by this phenomenon.[41] The sum of the first-order indices is 0.8, meaning that 20% of the variance in the model output is due to interactions between the input factors. The difference between S_i and S_{Ti} and a different ranking for both indices forms a measurement for nonlinearity. For S_i, the highest value corresponds to parameter β_2, followed by T_g and β_1, and here, the same conclusions are drawn as from the CSM plot, which was not the case for the SRCs or the SRRCs. Based on S_i, it can be concluded that $R_{w,0,fac}$ has almost no impact on the model output. As such, it can be concluded that due to the rank transformation the impact of $R_{w,0,fac}$ is erroneously increased. However, based on S_{Ti} the impact of $R_{w,0,fac}$ is not as low as indicated from the S_i, meaning that $R_{w,0,fac}$ is involved in interactions with other factors. As S_i equals 0.73 for β_2, this means that a reduction of 73% in the variance can be obtained if the value

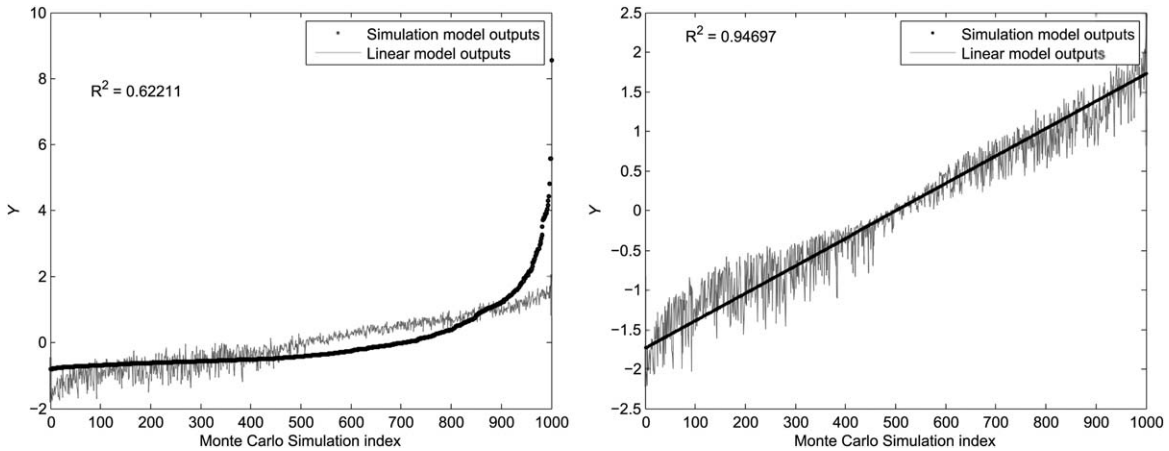

Figure 9. The linear regression of the output together with the simulated output [raw output (left) and rank transformed output (right)], where the input is generated using LHS sampling for the single particle drying model.

Table 5. Results of the Variance-Based Method for the Single Particle Drying Model

Parameter	S_i	S_{Ti}
T_g	0.0518	0.1553
p_g	−7.1411e-5	8.9759e-6
R_p	0.0021	0.0055
ε	2.6870e-7	2.4060e-4
M_w	0.0036	0.0013
ρ_{liquid}	1.2346e-4	0.0118
ρ_{solid}	0.0014	0.0033
β_1	0.0191	0.0593
β_2	0.7279	0.8543
$R_{w,0,fac}$	−3.7338e-4	0.0059
Sum	0.8	

for β_2 can be fixed. S_{Ti} is 0.85 for β_2, indicating the variance of β_2 alone and the fraction of variance explained by any combination of β_2 and the other factors.

As S_{Ti} for the factors p_g and ε equals almost zero, it means that both factors can be fixed anywhere in their range of variability without affecting the output. The fact that the porosity (ε) has almost no influence on the drying time is quite unexpected.

Comparison of Different GSA Techniques. In Table 6, the results of the different methods are summarized.It is clear that the computational effort is low for the Morris screening compared to the other techniques, for which the number of investigated factors is even decreased from 23 to 10. The ranking of the factors is also somewhat different; the ranking of the regression-based technique is obviously different compared to the other techniques. The rank transformation of the output ensures that the original output values are not used to calculate the sensitivity. As such, information is lost during this transformation, which can form an explanation for the different ranking. The difference between S_i and S_{Ti} is limited when looking at the ranking, but is more obvious when looking at the absolute values. This information is important to unravel which factors are responsible for nonlinearity.

When a GSA is used to perform a reduction of the full model, the suggestion is to choose the factors included in the analysis based on the goal of the reduced model. The reduction of the single particle drying model has been performed by Mortier et al.,[37] where the developed reduction scheme also includes a GSA. The objective was to use the PBM-model for simulating the evolution of the moisture content distribution in a fluidized bed drying unit, part of the ConsiGma™. Therefore, the factors are chosen based on the ability to adapt or control these factors during the operation of the dryer.[37] In this contribution, a more extensive GSA is performed including all factors in the model and the objective was to investigate the influence on the drying time, as well as to compare the different techniques in terms of performance and computational effort. For this reason, the outcome of the GSA has to be interpreted in another way. β_2 is the most sensitive factor, however, it has no physical interpretation. It is a coefficient introduced in the model during calibration. Due to it sensitivty, this factor is important during calibration, and when the model will be extended or recalibrated for other formulations, this information is important.

Table 6. Comparison of Different GSA Techniques for the Single Particle Drying Model

Technique	k	N	Most Sensitive Factors
Morris screening	23	240	β_2-T_g-β_1-$R_{w,0,fac}$
CSM plot	10	400	β_2- T_g-. . .
SRC	10	1000	–
SRRC	10	1000	β_2-$R_{w,0,fac}$-T_g-ρ_{solid}
S_i	10	1000	β_2-T_g-β_1-Mw
S_{Ti}	10	1000	β_2-T_g-β_1-ρ_{liquid}

PBM-model

Dotty Plots. One-dimensional dotty plots are created, which present the output of the GSA against the factor value, to understand the input–output relations. The dotty plots are created using 5000 samples generated by Sobol sampling. For both outputs, that is, μ_d and σ_d at the end of the process, a threshold value is selected. Below this value, the simulation is considered as "behavioral" (i.e., good with respect to chosen quality objective), whereas in the other case it is a "nonbehavioral" simulation. For the mean, a threshold value of 1.4% is selected, which is identical as in the case where a GSA is applied on the single particle drying model. For pharmaceutical applications, the granules do not need to have the same moisture content. A distribution of the granule moisture content at the end of the drying process is even beneficial for the subsequent tabletting step. The threshold value for the standard devation is therefore chosen as 0.1e-5.

The results for the mean are presented in Figure 11, and only the factors with a trend are visualized. It is obvious that a high gas temperature is beneficial to lower the moisture content, as the evaporation rate is higher. The lower the particle radius, the higher the evaporation, and as such the lower the mean moisture content. The influence of the gas velocity, the initial moisture content, and the filling time is marginal. The drying time has a more pronounced influence; however, also this factor is less important compared to the gas temperature and the particle radius.

Potential correlations between factors can be detected by constructing 2-D dotty plots (Figure 12). An even distribution of behaviorals and nonbehaviorals across the 2-D factor space means that both factors have no influence on the output, and no correlations between the factors can be detected. Looking at the dotty plot at the intersection of the particle radius and the drying time, it is obvious that a high value for the particle radius can be compensated by a high value for the drying time.

The same analysis can be made for the standard deviation of the distribution. In Figure 13, the results are presented for the factors with a trend, the y axis is logarithmic. The gas temperature has a clear influence on the final standard deviation: the higher the gas temperature, the faster the evaporation rate and the wider the distribution. The particle radius, the gas velocity, and the initial moisture content have no pronounced influence on the output. But whereas the filling time has no significant effect on the mean of the distribution, and as such on the evaporation rate, the influence on the standard deviation is obvious. The higher the filling time, the wider the distribution, which could be expected from experience. The influence of the drying time is quite limited: if the drying time is lower, the standard deviation seemed to be somewhat higher.

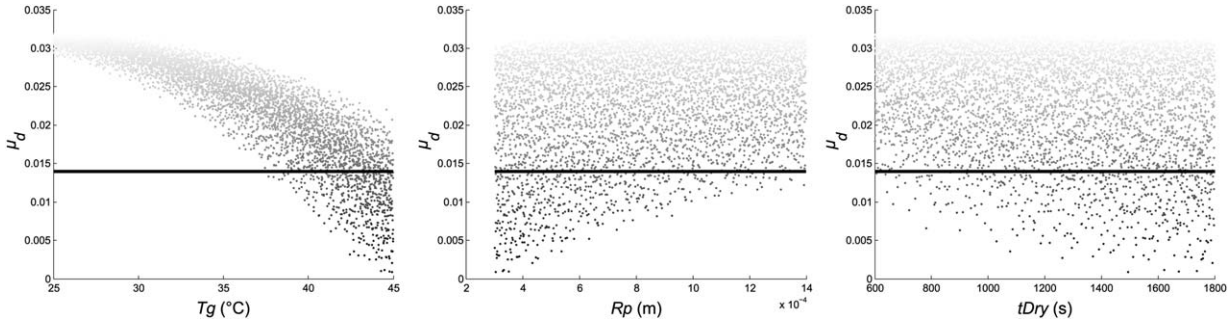

Figure 11. One-dimensional dotty plot of μ_d for the PBM-model.

The "behaviorals" are situated below the black line. The factors without any trend are not visualized.

The 2-D dotty plots for the final standard deviation of the number density distribution are interesting to detect correlations between the factors (Figure 14). A high value for the gas temperature can be compensated by a low filling rate, and the opposite is also valid. Again, it is clear that the influence of the drying time is limited: a somewhat higher drying time, combined with a higher gas temperature leads to a behavioral simulation, whereas also a high drying time and a high filling rate gives a behavioral combination.

Contribution to Sample Mean/Variance Plot. The data generated to create the dotty plots were further analyzed by creating CSM and CSV plots. The analysis was done using

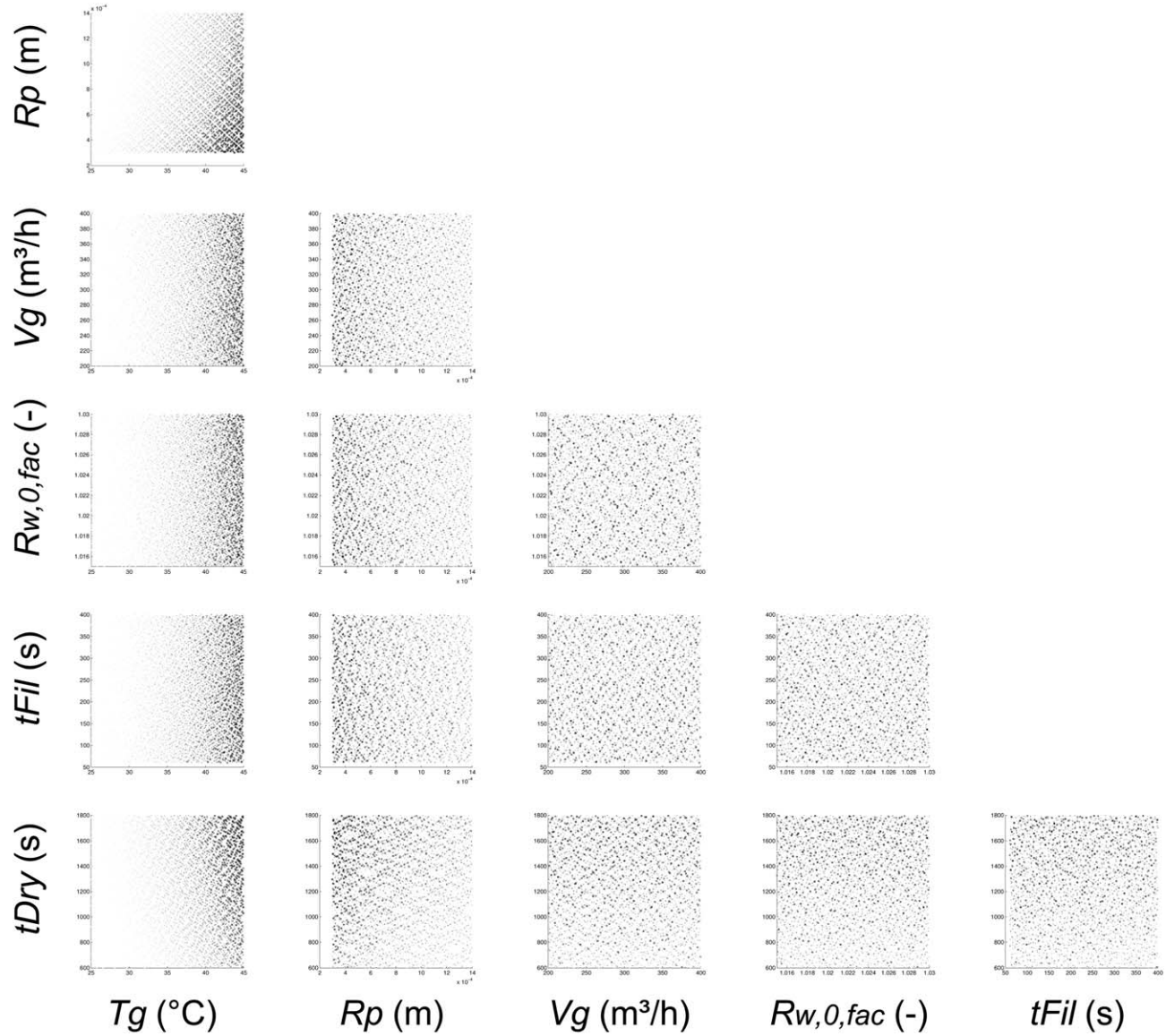

Figure 12. Two-dimensional dotty plots of μ_d for the PBM-model for all factor combinations.

Factor combinations with a low value for the mean are considered as behavioral.

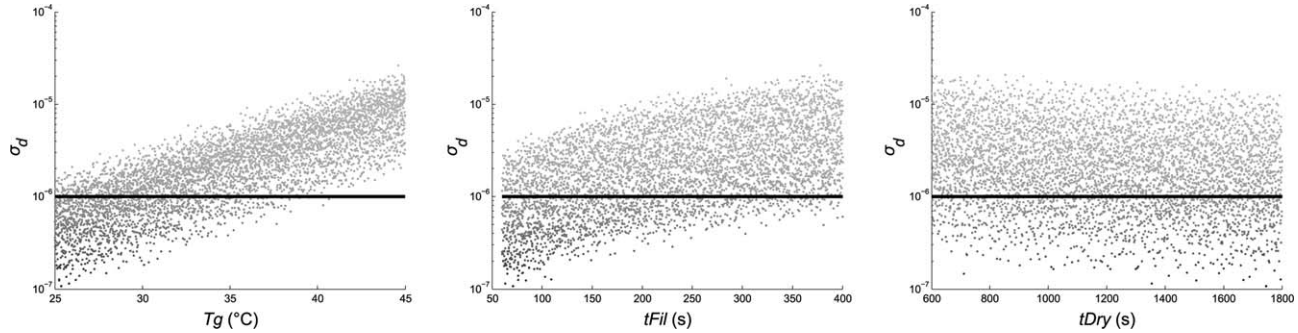

Figure 13. One-dimensional dotty plot of σ_d for the PBM-model.

The "behaviorals" are situated below the black line. The factors without any trend are not visualized. The *y* axis is logarithmic.

5000 samples. Based on the CSM, the particle radius is the most influential parameter, followed by the gas temperature (Figure 15). The concavity of the curves can be used to understand input–output relations. As the curve of the particle radius is situated below the bisector, this means that for increasing values of the particle radius the mean of the distribution increases. This could also be concluded based on the dotty plot (Figure 12). The mean of the distribution is the most unevenly distributed for the particle radius (Figure 15). The variance in the mean of the distribution is most

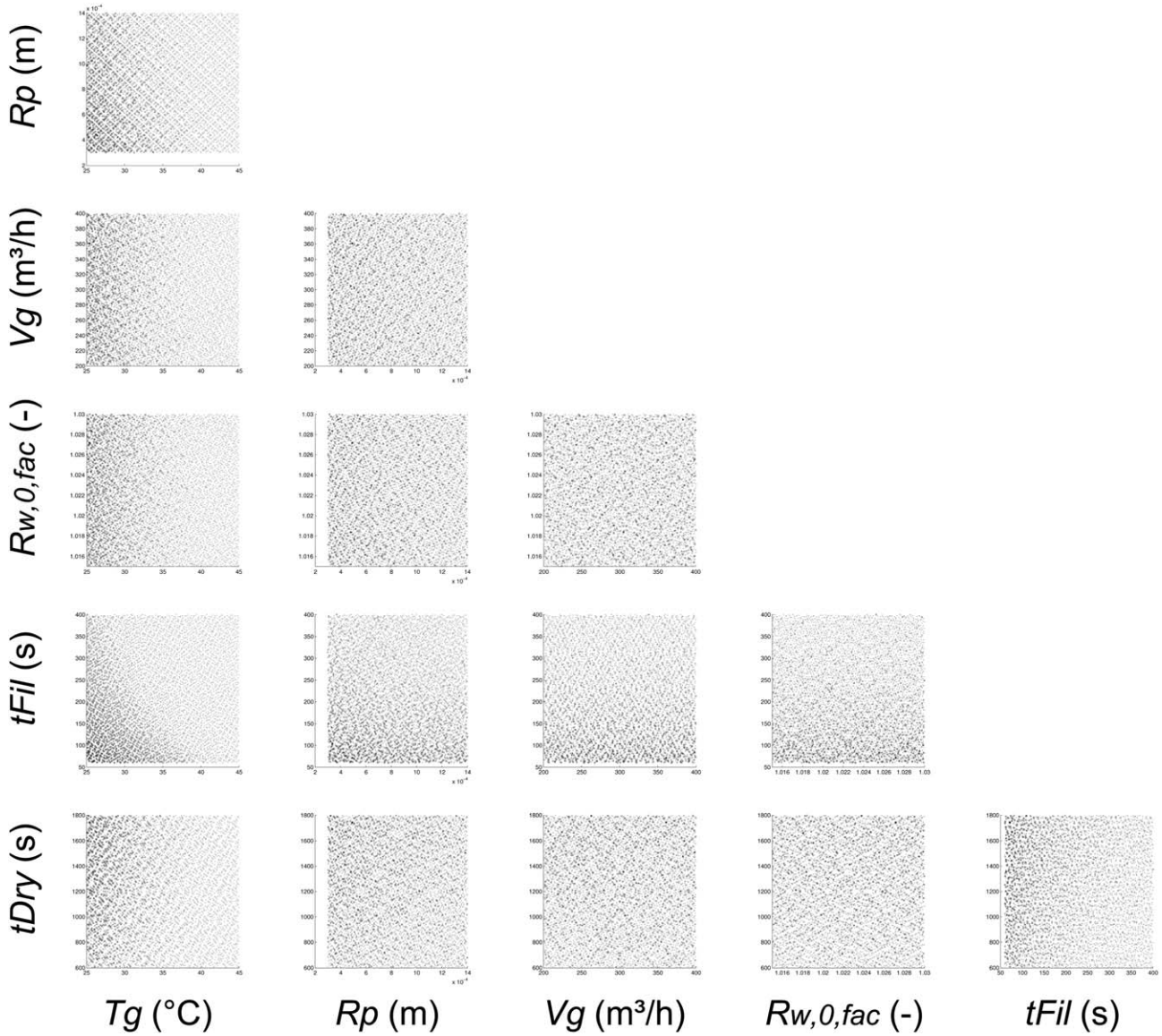

Figure 14. Two-dimensional dotty plots of σ_d for the PBM-model for all factor combinations.

Factor combinations with a low value for the mean are considered as behavioral.

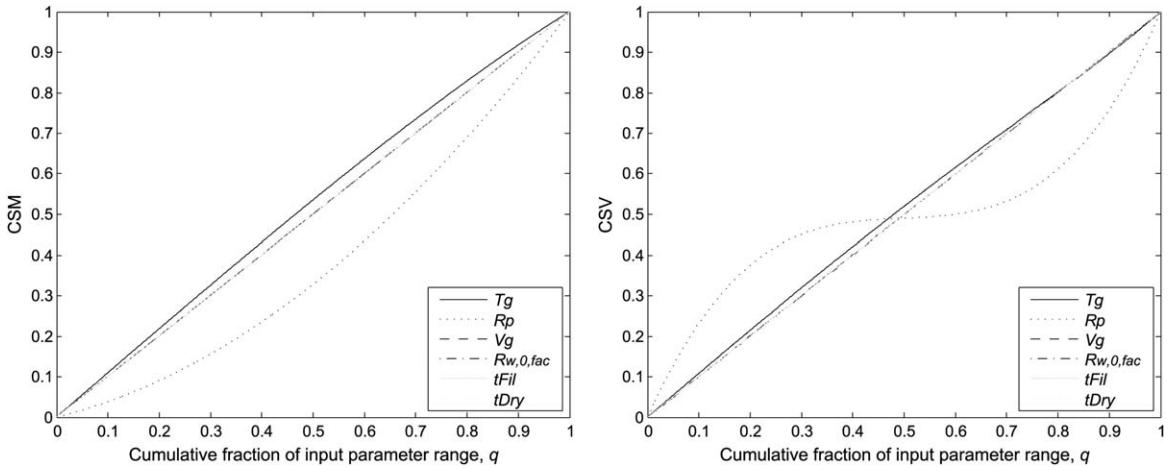

Figure 15. The CSM (left) and the CSV (right) plot of μ_d for the PBM-model using Sobol sampling.

pronounced for the particle radius, which is clearly visible in the dotty plot (Figure 14).

The standard deviation of the final distribution is most influenced by the gas temperature, followed by filling time (Figure 16). Also, the drying time and the particle radius are influential factors. Whereas an increasing value for the gas temperature leads to an increasing value for the standard deviation and increasing drying time decreases the width of the distribution. The variance is the most unevenly distributed for the gas temperature, followed by the filling time (Figure 16).

Regression-Based Sensitivity Analysis. The regression-based sensitivity analysis is performed with 5000 samples generated for the dotty plots. For the raw output data on the mean of the distribution an R_Y^2 of 0.99 is obtained, and the rank transformation has no influence on the coefficient of determination (0.99) (Table 7). R_p is clearly the most sensitive factor, followed by the gas temperature. The same conclusion could be drawn from the CSM plot. For the case with the standard deviation, the rank transformation has an effect on the coefficient of determination, however, in both cases the R_Y^2 is high enough to draw conclusions. The gas temperature is the most influential factor for the width of the distribution. In fact, the same order of significance is valid for the case with and without rank transformation for both outputs. But the difference between R_Y^2 for the standard deviation forms an indicator of the nonlinearity of the model. The SRRCs have no quantitative value compared to the SRCs, but can only be used to rank the input factors.

Variance-Based Sensitivity Analysis. The sensitivity indices, computed based on the method proposed by Saltelli et al.,[34] are presented in Table 8. For this analysis, 1000 samples were generated. The sum of S_{i,μ_d} corresponds to 0.99, which indicates that the input factors as such are responsible for almost all variance in the model output. The particle radius is obviously the most sensitive factor, and the same conclusion could be drawn for the CSM plot. The gas temperature has a limited effect on the mean moisture content.

The sum of the first-order indices is 0.86 for the standard deviation, meaning that interactions between the input factors are responsible for only 14% of the variance in the model output. For S_{i,σ_d} the highest value corresponds to parameter T_g, followed by t_{fill}. The sensitivity of t_{dry} and R_p is somewhat comparable. The same conclusions could be drawn as from the CSV plot. Taking interactions between factors into account, still T_g is the most important factor. As the difference between S_{i,σ_d} and S_{Ti,σ_d} is low for t_{dry}, this

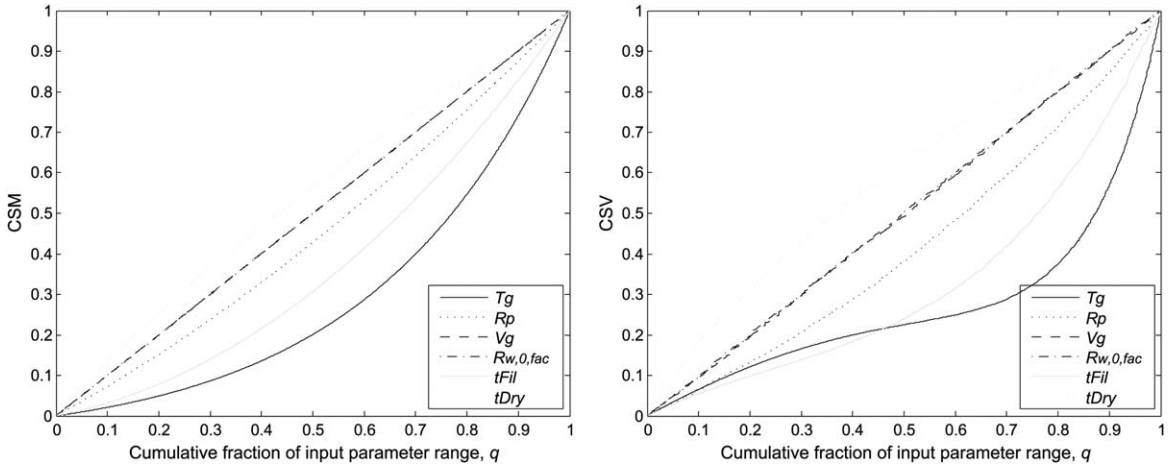

Figure 16. The CSM (left) and the CSV (right) plot of σ_d for the PBM-model using Sobol sampling.

Table 7. Results of the Regression-Based Method for the PBM-Model

Parameter	SRC_{μ_d}	$SRRC_{\mu_d}$	SRC_{σ_d}	$SRRC_{\sigma_d}$
T_g	0.2034	0.1953	0.7211	0.8184
R_p	0.9738	0.9751	0.1700	0.1805
V_g	2.4961e-4	2.4058e-4	5.0140e-4	4.6201e-4
$R_{w,0,fac}$	2.1012e-4	3.5198e-5	0.0016	0.0017
t_{fil}	0.0078	0.0074	0.4527	0.4926
t_{dry}	0.0540	0.0517	0.1583	0.1531
R_Y^2	0.99	0.99	0.78	0.97

Table 8. Results of the Variance-Based Method for the PBM-Model

Parameter	S_{i,μ_d}	S_{Ti,μ_d}	S_{i,σ_d}	S_{Ti,σ_d}
T_g	0.0441	0.0495	0.5900	0.7245
R_p	0.9451	0.9488	0.0322	0.0521
V_g	−7.2737e-7	7.5451e-8	−3.3177e-5	1.3572e-6
$R_{w,0,fac}$	−9.1197e-6	3.7276e-7	7.7727e-5	5.5935e-6
t_{fil}	7.7140e-5	9.9028e-5	0.1923	0.3434
t_{dry}	0.0030	0.0047	0.0462	0.0506
Sum	0.9921		0.8607	

factor is almost not involved in interactions with other factors. This is reasonable, as the drying time indicates only the end of the drying process, but has no influence on the process itself.

Comparison of Different GSA Techniques. In Table 9, the results of the different methods are summarized. The ranking is identical for all techniques. As the data to create the dotty plots is further used for the CSM and CSV plots and the regression-based analysis, the same amount of samples is used, that is, 5000 samples. For the variance-based analysis only 1000 samples are used.

The mean of the moisture content distribution is mostly influenced by the particle radius of the granules. However, this factor is primarily determined by the preceding unit process, that is, the granulation step. The gas temperature is also influential, and has both an effect on the mean value as well as the range of the distribution. As such, this factor is the key to control the specs of the distribution during operation, and should be included in a control strategy to ensure that the final quality of the dried product meets the specifications.

Discussion

The different GSA techniques obviously have advantages and disadvantages. A strong limitation of the methods is the requirement to choose one single output value of interest. The result will in any case by dependent on the selection of this output value. When one is only interested in the end quality of the product, one can choose an end point as output value. However, when one wants to monitor and control a process based on the information obtained by a GSA, the mean of a simulated time series or another point during transient conditions can be chosen.

The Morris screening is an interesting technique to start with when a lot of factors are involved in the analysis. A differentiation between less and more important factors can be made without the need for a lot of samples, which limits the analysis time. Graphical tools are useful to detect input–output relations, and dotty plots give basic information about trends (i.e., positive or negative correlations) and the standard deviation of the output. The CSM/CSV plots give the same information, but are also useful to rank factors.

Table 9. Comparison of Different GSA Techniques for the PBM-Model

Technique	k	N	Most Sensitive Factors for μ_d	Most Sensitive Factors for σ_d
CSM plot	6	5000	R_p-T_g	T_g-t_{fil}
SRC	6	5000	R_p-T_g	T_g-t_{fil}
SRRC	6	5000	R_p-T_g;	T_g-t_{fil}
S_i	6	1000	R_p-T_g	T_g-t_{fil}
S_{Ti}	6	1000	R_p-T_g	T_g-t_{fil}

The regression-based sensitivity analysis is an often used technique; however, the assumption of linearity is a serious drawback. Performing a rank transformation on the simulated output can be a solution, where the difference between the R_Y^2 of the linear regression is an indicator for the nonlinearity of the model. Also, this method requires significantly more simulations compared to the graphical tools.

The variance-based sensitivity analysis has the same computational effort compared to regression-based sensitivity analysis, but more information is obtained. By calculating the sum of the sensitivity indices, the variance explained by the factors, included in the analysis, is known. The difference between the first-order effect (S_i) and the total effect (S_{Ti}) is an indication for nonlinearity.

To conclude for a model with a lot of factors, it is recommended to start with the Morris screening to eliminate part of the factors in further analyses which require more computational effort. The variance-based sensitivity technique is the best option to obtain as much information as possible about the model.

The results for the single particle drying model show that β_2 is the most influential factor. This is an important aspect when performing a model calibration and the same is valid for β_1. However, both factors have no physical meaning and were introduced during calibration of the single particle drying model. The significant influence of the gas temperature T_g is of interest when performing experiments or using the equipment during the production of pharmaceutical tablets. If for instance the set point of the gas temperature does not match with the real gas temperature, the drying time will be inaccurately predicted by the model. The fact that the gas velocity has no influence on the drying time gives the operator the possibility to use this input factor to control the fluidization of the particles without disturbing the drying behavior.

During operation of the ConsiGma™, the dryer unit is filled with a batch of particles. To control the moisture content of the granules leaving the dryer, the operator should play with the particle radius and the gas temperature. The particle radius is obviously an input to the drying process and should be controlled by the granulator prior to the drying step. However, the range in moisture content of the dry granules can be altered by adapting the filling time. As the gas temperature has also a significant impact on the moisture interval, and a balance should be found between the drying time and the interval when changing the gas temperature

during operation. Furthermore, for a population of granules, the gas velocity has no influence on the drying behavior, neither on the mean moisture content nor on the interval in moisture content, and as such, it can only be used to control the fluidization behavior of the granules.

Conclusions

Different GSA techniques are compared for two models: (1) the single particle drying model for pharmaceutical granules using one output, that is, the time to reach a moisture content of 1.4% and (2) a PBM-model to describe the drying behavior of pharmaceutical granules in the ConsiGma^{TM}.

An important remark is that the used methods can be computationally expensive (depending on the model complexity), but are easy to automate toward other cases. Based on the results, it is suggested to start with a Morris screening when the model consists of a lot of factors. Afterward, a variance-based sensitivity technique can be performed, which provides a lot of information about the model and the underlying process.

The most sensitive factor for the single particle drying model is β_2, and thus this factor is important for model calibration to reduce output uncertainty.

For the PBM-model, the particle radius has a large influence on the drying rate; however, this factor is mostly determined by the granulation step. Conversely, the gas temperature, which is also an influential factor, can be used to direct the process during operation as it has influence on both the mean moisture content, as well as on the width of the moisture content distribution. The interval in moisture content is also determined by the filling time.

Acknowledgment

Financial support for this research from the Fund for Scientific Research Flanders (FWO Flanders – Ph.D. fellowship Séverine Thérèse F. C. Mortier) is gratefully acknowledged.

Literature Cited

1. Leuenberger H. New trends in the production of pharmaceutical granules: batch versus continuous processing. *Eur J Pharm Biopharm*. 2001;52:289–296.
2. Plumb K. Continuous processing in the pharmaceutical industry: changing the mind set. *Chem Eng Res Des*. 2005;83:730–738.
3. Mortier STFC, De Beer T, Gernaey KV, Remon JP, Vervaet C, Nopens I. Mechanistic modelling of fluidized bed drying processes of wet porous granules: a review. *Eur J Pharm Biopharm*. 2011;79: 205–225.
4. Jakeman AJ, Letcher RA, Norton JP. Ten iterative steps in development and evaluation of environmental models. *Environ Model Softw*. 2006;21:602–614.
5. Saltelli A, Tarantola S, Campolongo F, Ratto M. *Sensitivity Qnalysis in Practice: A Guide to Assessing Scientific Models*. Chichester: Wiley, 2004.
6. Saltelli A, Ratto M, Tarantola S, Campolongo F. Sensitivity analysis for chemical models. *Chem Rev*. 2005;7:2811–2828.
7. Cacuci DG, Ionesco-Bujor M. A comparative review of sensitivity and uncertainty analysis of large-scale systems - II: statistical methods. *Nucl Sci Eng*. 2004;147:204–217.
8. Saltelli A, Ratto M, Andres T, Campolongo F, Cariboni J, Gatelli D, Saisana M, Tarantola S. *Global Sensitivity Analysis: The Primer*. Chichester: Wiley, 2008.
9. Pappenberger F, Iorgulescu I, Beven KJ. Sensitivity analysis based on regional splits and regression trees (SARS-RT). *Environ Model Softw*. 2006;21:976–990.
10. Campolongo F, Saltelli A, Cariboni J. From screening to quantitative sensitivity analysis. A unified approach. *Comput Phys Commun*. 2011;182:978–988.
11. Campolongo F, Cariboni J, Saltelli A. An effective screening design for sensitivity analysis of large models. *Environ Model Softw*. 2007; 22:1509–1518.
12. Morris MD. Factorial sampling plans for preliminary computational experiments. *Technometrics*. 1991;33:161–174.
13. Sobol' IM. On quasi-Monte Carlo integrations. *Math Comput Simul*. 1998;47:103–112.
14. Giunta AA, Wojtkiewicz SF Jr, Eldred MS. Overview of modern design of experiments methods for computational simulations. *41st AIAA Aerospace Sciences Meeting and Exhibit*. Albuquerque, NM, 2003:1–17.
15. Koehler JR, Owen AB. Computer experiments. Handbook of Statistics. New York: Elsevier Science, 1996:261–308.
16. Diwekar UM, Kalagnanam JR. Efficient sampling technique for optimization under uncertainty. *AIChE J*. 2004;43:440–447.
17. McKay MD, Beckman RJ, Conover WJ. A comparison of three methods for selecting values of input variables in the analysis of output from computer code. *Technometrics*. 2000;42:55–61.
18. Minasny B, Bratney AB. A conditioned Latin hypercube method for sampling in the presence of ancillary information. *Comput Geosci*. 2006;32:1378–1388.
19. Sobol' IM. On the systematic search in a hypercube. *SIAM J Numer Anal*. 1979;16:790–793.
20. Halton JH. On the efficiency of certain quasi-random sequences of points in evaluating multi-dimensional integrals. *Numer Math*. 1960; 2:84–90.
21. Faure H. Discrepance de suites associees a un systeme de numeration (en dimensions). *Acta Arith*. 1982;41:337–351.
22. Hammersley JM. Monte Carlo methods for solving multivariate problems. *Ann NY Acad Sci*. 1960;86:844–874.
23. Sobol' IM, Kucherenko SS. On global sensitivity analysis of quasi-Monte Carlo algorithms. *Monte Carlo Methods Appl*. 2005;11:83–92.
24. Tarantola S, Becker W. A comparison of two sampling methods for global sensitivity analysis. *Comput Phys Commun*. 2012;183:1061–1072.
25. Sobol' IM. Uniformly distributed sequences with an additional uniform property. *USSR Comput Math Math Phys*. 1976;16(5):236–242.
26. Tarantola S, Kopustinskas V, Bolado-Lavin R, Kaliatka A, Uščuras E, Vaišnoras M. Sensitivity analysis using contribution to sample variance plot: application to a water hammer model. *Reliab Eng Syst Saf*. 2012;99:62–73.
27. Sinclair JE. Response to the PSACOIN level s exercise. PSACOIN Level S Intercomparison. Paris: Nuclear Energy Agency (NEA) (OECD), 1993:138–158.
28. Bolado-Lavin R, Castaings W, Tarantola S. Contribution to the sample mean plot for graphical and numerical sensitivity analysis. *Reliab Eng Syst Saf*. 2009;94:1041–1049.
29. Helton JC. Uncertainty and sensitivity analysis techniques for use in performance assessment for radioactive waste disposal. *Reliab Eng Syst Saf*. 1993;42:327–367.
30. Urbonas R, Kaliatka A, Kopustinskas V. Comparative sensitivity study of the RBMK-1500 reactor one group distribution header blockage accident model. *Nucl Eng Des*. 2010;240:3238–3247.
31. Saltelli A. *The Critique of Modelling and Sensitivity Analysis in the Scientific Discourse: An Overview of Good Practices*. Washington: TAUC, 2006.
32. Homma T, Saltelli A. Importance measures in global sensitivity analysis of nonlinear models. *Reliab Eng Syst Saf*. 1996;52:1–17.
33. Saltelli A, Tarantola S. On the relative importance of input factors in mathematical models: safety assessment for nuclear waste disposal. *J Am Stat Assoc*. 2002;97:702–709.
34. Saltelli A, Annoni P, Azzini I, Campolongo F, Ratto M, Tarantola S. Variance based sensitivity analysis of model output. Design and estimator for the total sensitivity index. *Comput Phys Commun*. 2010; 181:259–270.
35. Jansen MJW. Analysis of variance designs for model output. *Comput Phys Commun*. 1999;117:35–43.
36. Mortier STFC, De Beer T, Gernaey KV, Vercruysse J, Fonteyne M, Remon JP, Vervaet C, Nopens I. Mechanistic modelling of the drying behaviour of single pharmaceutical granules. *Eur J Pharm Biopharm*. 2012;80:682–689.
37. Mortier STFC, Van Daele T, Gernaey KV, De Beer T, Nopens I. Reduction of a single granule drying model: an essential step in

preparation of a PBM with a continuous growth term. *AIChE J*. 2013;59:1127–1138.
38. Mortier STFC, Gernaey KV, De Beer T, Nopens I. Development of a population balance model of a pharmaceutical drying process and testing of solution methods. *Comput Chem Eng*. 2013;50:39–53.
39. Qamar S, Warnecke G. Numerical solution of population balance equations for nucleation, growth and aggregation processes. *Comput Chem Eng*. 2007;31:1576–1589.
40. Crosetto M, Tarantola S. Uncertainty and sensitivity analysis: tools for GIS-based model implementation. *Int J Geogr Inf Sci*. 2001;15:415–437.
41. Archer GEB, Saltelli A, Sobol IM. Sensitivity measures, anova-like techniques and the use of bootstrap. *J Stat Comput Simul*. 1997;58:99–120.

Manuscript received Aug. 22, 2013, and revision received Dec. 5, 2013.